



Article Processing Dates: Received on 2022-12-27, Reviewed on 2023-02-17, Revised on 2023-02-27, Accepted on 2023-02-03, and Available online on 2023-04-28

Effect of full annealing and single quenching-tempering heat treatment on the mechanical properties of JIS SUP 9A steel

Andreas Luki Indratmoko, Irza Sukmana, Mohammad Badaruddin*

Magister Program Study of Department of Mechanical Engineering, University of Lampung, Bandar Lampung, 35145, Indonesia

*Corresponding author: mbruddin@eng.unila.ac.id

Abstract

JIS SUP 9A leaf spring steel under hot-forging conditions was subjected to Full Annealing (FA) and Single Step-Quenching-tempering heat treatments (SQT). Tensile test specimens to ASTM E 8 standards have been prepared. The FA process was performed by heating all specimens in the furnace at a constant temperature of 800°C for 2 hours, followed by cooling in the furnace. Then, all test specimens were heat-treated SQT. The SQT process was carried out by heating all samples in a furnace at 800°C for 1 hour and 650°C for 1 hour, each followed by immersion in Crude Palm Oil (CPO) media at a liquid temperature of 70°C until the specimens reached 100°C. The FA process removed internal stresses with high microstructural softness and SQT produces a fine martensitic phase microstructure, which improves mechanical strength (tensile strength and impact strength) with good ductility. Electron and scanning microscopy have been used to determine the concentration of impurities and microstructural changes in relation to the mechanical properties of the specimen concerned. The results showed that the yield limit, maximum tensile stress, and impact energy increased by 113.5%, 16.3%, and 705.2%, respectively. However, hardness decreased by 18.8% for SQT specimens against FA after heat treatment. This research utilizes industrial waste, which is available quite a lot; in the future, it will become an alternative for handling environmental problems. The abundant availability of raw materials and resulting strength-toughness are the main advantages of this heat treatment.

Keywords: Leaf spring steel, full annealing, single quenching tempering, crude palm oil, mechanical strength.

1 Introduction

Many material and design engineers are interested in medium and low alloy steel as materials applied in the industrial world because they are easy to maintain, and the price is relatively low compared to other alloyed carbon steels. Increasing the mechanical strength of low-alloy carbon steel is generally carried out through a quenching process which followed by a tempering process [1]. Therefore, low alloy carbon steel is often applied to engineering components, such as excavator bucket materials, disc plows, slashers, and cane cutters [2]. The steel can resist frictional loads

during the process of dredging the soil, plowing the land and trimming the sugar cane. High quality steel is generally produced using the TMCP (Thermo Mechanical Control Process) method, that combines casting processes, rolling and controlled heat treatment in one process line [3]. This non-simple and complicated manufacturing process causes the high price of high-quality steel.

Compared to the TCMP process, conventional heat treatment of carbon steel using the Single Quenching-Tempering (SQT) method is more beneficial for producing a good balance of strength-toughness, reduced energy consumption, shorter processing times and lower costs for the manufacture of wear-resistant steel [4, 5, 6]. The austenization of low alloy carbon steel followed by quenching-tempering process is widely applied in microstructural engineering to obtain material components with relatively high mechanical strength and suitable ductility.

JIS SUP 9 steel has mechanical and thermal properties, as seen in Table 1. The test used truck leaf springs that had undergone a cold rolling process and generally had high tensile strength, good elastic strength, and better corrosion resistance than carbon steel [7].

FA heat treatment is required to remove internal stresses and refine the microstructure. The researchers want to make sure that this steel is used for the sugarcane blades so that in advance, the spring steel is straightened by the hot forging process. Additionally, before quenching and tempering, the steel is first annealed to ensure the microstructure of the steel is only pearlite and ferrite. JIS-SUP-9 similarity in international standardization: Chinese standard (GB) 55CrMnA, American standard (ASTM) 5155, French standard (AFNOR) 55C3, European standard (EN) 55Cr3, and British Standard (BS) 525A58 & 525H60. SUP-9 is specially used to manufacture leaf springs for locomotives, and carriages [9, 10].

Heat treatment can increase the strength of low alloy steels through controlled heating and cooling procedures that induce specific properties into the steel [11]. Heat treatment of steel is intended to improve the mechanical properties of steel by changing the size and micro shape of its constituents (phase structure) [12, 13]. By changing the microstructure, the alteration of the mechanical properties steel significantly increase. For this reason, evaluation of strength (tensile and impact-toughness) is an important content in the failure-safe design of materials to be carried out.

This study followed the heat treatment process by a tempering process using CPO (Crude Palm Oil) cooling medium. The manufacturing process begins with hot forging so that the ex-spring material becomes flat and does not warp, followed by full annealing (FA) and a single quenching-tempering (SQT) process. This quenching process develops the α' phase of saturated carbon while further tempering decomposes the excess α' phase carbon into the remaining γ phase [14]. The transformation of the lath martensite during the SQT process divides the previous γ grains into packets and divides each pack into parallel batten blocks. Since the packages and beams have large corner angles, this is considered to have a significant effect on the mechanical properties of the steel [15].

2 Experimental Materials and Procedures

2.1 Material Preparation

This research was conducted at the University of Lampung's Mechanical Engineering Materials Laboratory, while the testing site was at the Tanjung Bintang Mineral Development Center, South Lampung. This test specimen was made by machining process from JIS SUP 9A alloy steel in used condition with a thickness of 15 mm and a width of 80 mm and is industrial waste at PT Gula Putih Mataram-Lampung Tengah with the chemical composition given in Table 2.

Table 1. Mechanical and thermal properties of JIS SUP 9A material [8].

Mechanical Properties	Elastic Modulus (GPa)	Poisson Ratio	Tensile Strength (MPa)	Yield Strength (MPa)	Shear Modulus (Gpa)
	190	0,29	1225	1080	73
Thermal Properties	Melting Point (°C)	Specific Heat Capacity (J/kg-K)	Thermal Conductivity (W/m-K)	Thermal Expansion (µm/m-K)	
	1450	470	48	13	

Table 2. Chemical composition of the present JIS SUP 9A investigated (wt.%).

%C	%Si	%Mn	%P	%S	%Cr	%Mo	%Fe
0.5597	0.3540	0.9111	0.0155	0.0179	0.9287	0.0024	Bal.

2.2 Materials and Test Equipment

In this study, the quenching media used CPO (Crude Palm Oil) with a liquid temperature of 70°C until the test object reached a temperature of 100°C within 3 minutes Fig 2. And the austenitization process used the Naberthem box furnace. The initial temperature of the CPO media was maintained at 70°C. The temperature selection of 70°C was determined based on the predictable starting point of martensite formation using the Bhadeshia software [3]. Impact tester Charpy, portable hardness tester Leeb Hardness Tester model AR936 and MTS Landmark 100 kN tensile tester were used. The CPO oil quenching media was heated in a stainless-steel tub with a diameter of 5 inches and a height of 400 mm with a capacity of 4.3 liters, using a 3 kW silica heater and the temperature of the oil bath was controlled using a Type K thermocouple (XCIB from Omega USA) with an autonic controller. The machining process for making mechanical testing specimens used a CNC Feeler FTC 350 XL and a CNC Feeler VMP 40A made in Taiwan.

2.3 Heat Treatment Process

The FA and SQT processes on hot forging leaf spring steel schematically can be seen in Fig. 1. JIS SUP 9A (Table 1.) with mechanical and thermal properties includes C=0.5597% hypo-eutectoid steel, FA sample is 25°C to 50°C higher than A3 transformation. It is heated to the austenite temperature for some time—800°C maximum for 120 minutes, followed by slow cooling in a furnace [16]. Austenitized to 800°C and held for 60 minutes followed by cooling the hot CPO oil to 70°C until the specimen reached 100°C. The SQT heat-treated specimens were finished by tempering at 650°C for 60 minutes, followed by cooling the CPO oil using the same quenching method as the FA specimens to achieve high levels of tensile strength and toughness. In heat treatment with an authentication temperature of 880°C and tempering of 560°C, martensite and finer grains have started to form. [17].

2.4 Test Method

Mechanical properties including tensile strength, elongation, reduction of cross-sectional area, V-notch impact energy and wear resistance are shown from the description of the three heat treatment observations respectively.

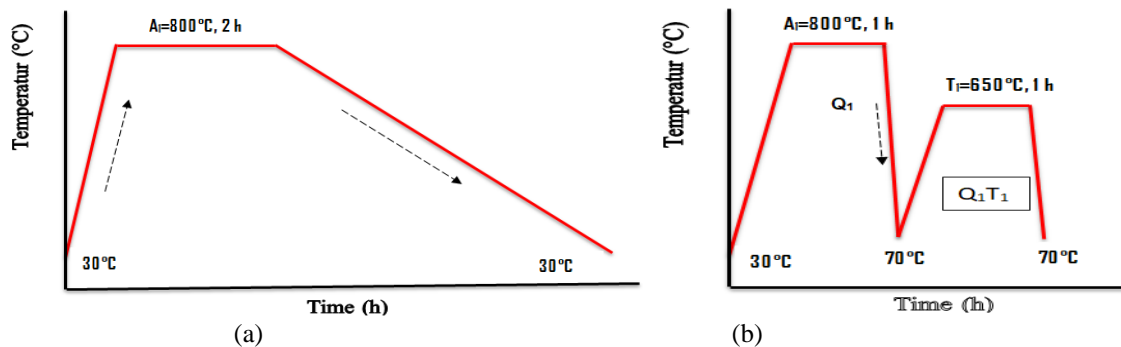
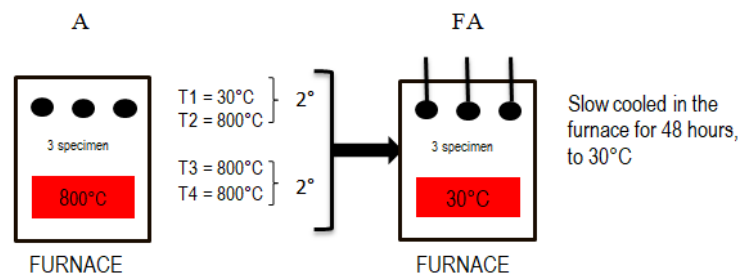


Fig. 1. Work steps of the heat treatment process: (a) FA and (b) SQT.



Heat Treatment Time 52 hours, Test Code FA.

(a)

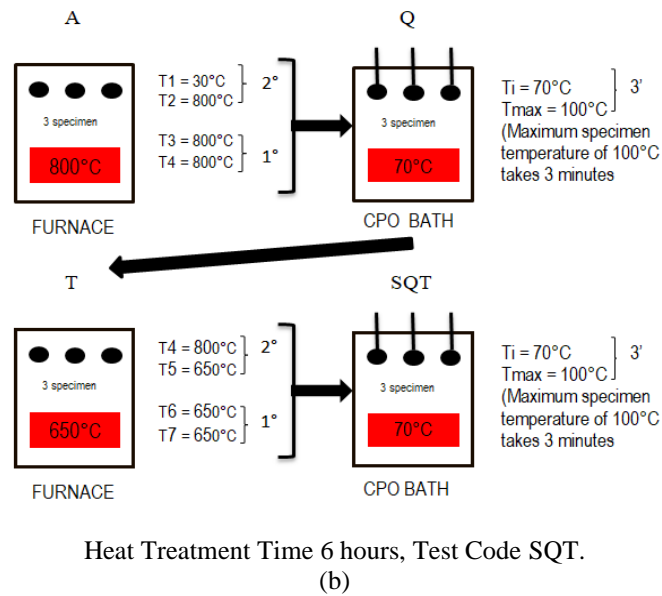


Fig. 2. Heat treatment process flow on specimen; (a) Full Annealing (FA) Process Flow, (b) Single Quenching Tempering (SQT) Process Flow.

Hardness measurement used the Rockwell method and reported as the RB hardness number according to ASTM E18 [18]. The shape and size dimensions of the tensile test specimens were prepared according to ASTM E8 standards [19] for tensile testing using a 100 kN MTS Landmark machine. Room temperature Charpy V-notch impact testing was carried out with the shape and dimensions of the specimen according to ASTM E23 standard [20]. Specimen preparation for microstructure testing and formed phases was carried out using SEM and EDS according to ASTM E2809-13 standard [21].

Tensile testing at room temperature with the first axial movement control of the actuator used a constant strain rate of 0.3%/min to determine the material's resistance to elastic deformation and the limit of the material deforming without additional load (0.2% offset). After the specimen reaches 0.3% strain, the actuator control is automatically switched to displacement control at a 3.5 mm/min speed [22]. The test was carried out until the specimen broke.

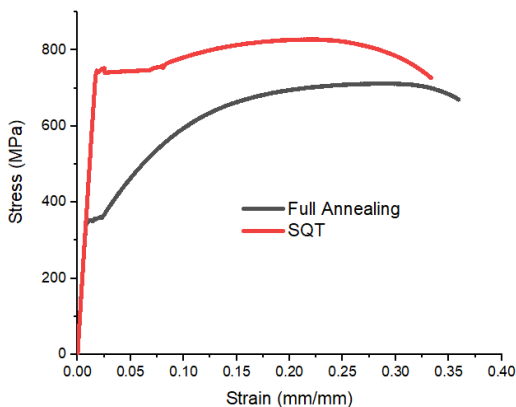


Fig. 3. Stress-strain behavior in FA and SQT specimens.

The hardness test performed on each specimen is five points of emphasis. There are 6 specimens that will be tested for hardness, so there is a total of 30 pressure points that will take the average value for each specimen. The portable hardness tester Leeb Hardness Tester model AR936 is used, has a working principle whereby tungsten carbide becomes a spherical test indenter which will be pounded on the surface of the specimen with a spring force. The impact speed of the colliding object will pass through and induce

the coil and the speed of the magnet goes according to the incoming electric voltage, so the screen will display the hardness value.

3 Results and Discussion

3.1 Mechanical Properties

The stress-strain curve (σ - ϵ) of the FA and SQT test materials is shown in Fig. 3. Likewise, the maximum elongation and reduction in fracture area of the FA and SQT specimens are shown in Table 3. The results of measurements of the V-notch impact energy test, Rockwell-B hardness and grain size in the fracture area are also listed in Table 3. From the results of this investigation, it was found that the tensile strength results of SQT specimens were higher than the FA specimen and the ductility value.

The ductile consistency for this treatment is inversely proportional to the grain size; the more significant the grain size, the lower the flexibility, and vice versa. The SQT impact test results show a substantial improvement in toughness compared to FA. In the FA heat treatment process, many corrugated lamellar cracks (pearlite area) and dimples (ferrite area) can first be seen on the surface of the damage, Fig 4a. The dimpled area gradually consumes the entire fault surface, and the flattened area of the fracture gradually removed by SQT heat treatment Fig 4b. [23].

This is also evident in the nearly 12-fold refinement of the developed austenite grains in the SQT sample. Initially, the strength properties were improved mainly by better micro components (ferrite and pearlite). After that, it was slightly reduced by removing flat and raised pearlite cementite balls in the structure. Thus, the ferrite-martensite process occurs, and the toughness increases with SQT heat treatment [23]. The difference in hardness values is also shown in Table 3. The trend of hardness values after hardening decreased in samples that underwent FA heat treatment.

Table 4 describes the tensile test of full annealing and single quenching-tempering heat treatment with each 3 specimens. That from the tensile test it is known that the SQT material has a higher mechanical property value compared to the annealing material. This is due to the formation of a finer grain structure which causes an increase in the strength of its mechanical properties. Standard deviation is done to find out the standard deviation between each specimen. The value of the standard deviation is a value that is used to determine the distribution of data in a sample and see how close the data is to the mean value.

Table 3. The mechanical properties obtained from the present investigation.

Heat treatment	0,2% Yield Strength (Mpa)	Ultimate Tensile Strength (Mpa)	Elongation (%)	Reduction in area (%)	Impact Energy (J)	Hardness (RB)	Grain size (µm)
FA	348,98	712,13	28,19	22,27	13,33	89,22	56,84
SQT	744,96	828,32	29,42	37,68	107,33	75,11	4,87

Table 4. STDEV on tensile test results for Full Annealing and Single Quenching-Tempering heat treatment.

Heat Treatment	0,2% Yield Strength (MPa)	Ultimate Tensile Strength (MPa)	Modulus Elastisitas (GPa)	Elongation (%)	Reduction in area (%)
FA 1	344,79	699,05	86,61	28,68	42,61
FA 2	355,81	727,96	100,12	27,74	37,24
FA 3	348,94	712,99	102,37	28,14	38,87
STDEV	5,56	14,45	8,52	0,47	2,75
SQT 1	723,04	816,50	158,94	26,98	61,85
SQT 2	754,29	838,09	125,55	31,58	62,11
SQT 3	755,93	837,58	132,34	29,71	59,50
STDEV	18,53	12,32	17,65	2,31	1,44

The standard deviation described in Table 4 is the best measure of spread because it represents the magnitude of the space for each unit of observation. From the discussion it can be concluded that the UTS value of annealing specimens 1 to 3 has a large enough deviation. This result is due to the influence of the physical properties of the material and the heat treatment process which is not very homogeneous due to the use of material from JIS SUP 9A leaf spring waste as well as for the yield deviation value, the smaller the STDEV value, the more homogeneous the material.

3.2 Fractographical Observation

SEM fractography was investigated from impact test specimens from Full Annealing (FA) and Single Quenching-Tempering (SQT) heat treatment. SEM analysis surfaces can be analyzed with SEM magnification up to 10,000x. Fig. 4 shows the 2,000x magnification at 0 mm spacing of the fractured impact specimen obtained by applying the FA and SQT processes. The FA specimen was carried out by heating in a furnace at a temperature of 800°C held for 120 minutes, then slow cooling in the furnace. This FA heat treatment process resulted in an increase in the number of micro void failures compared to the SQT heat treatment.

In addition, it is believed that the small local plastic stresses and primarily concentrated stresses in the martensite phase cause rapid microcracking; As a result, many sub-cracks are formed at the ferrite-martensite interface, as shown in Fig. 5a, which accelerates crack propagation [24]. Meanwhile, the SQT specimen was heated in a furnace at 800°C and 650°C, held for each 60 minutes, then quenched in CPO medium at 70°C until the specimen temperature was 100°C.

It can be seen in Fig. 5 that the crack occurs in the middle of the notch end until it spreads towards the center of the impact load. At the micro observation scale, the cracking process in JIS SUP 9A metal generally occurs in the first phase, beginning with the growth of micro voids or cracks, after which local failure occurs and in the second phase, oxides, inclusions or impurity particles are formed and precipitates are formed [25].

FA material is a material that is quite brittle because the grain boundaries are still quite large. The fracture surface is permanently deformed, marked by the appearance of a large number of dimples. The amount of displacement at the grain boundaries, directly or indirectly greatly affects the formation of dimples [16].

The grain measurements are also given in Fig. 6. From these values it can be seen that the grain size of the SQT specimen increased by almost 12 times finer than that of the FA specimen. Correspondingly, the size of the martensite packets was found to increase in number after the SQT conditions were also confirmed by the SEM micrographs in Fig. 6.

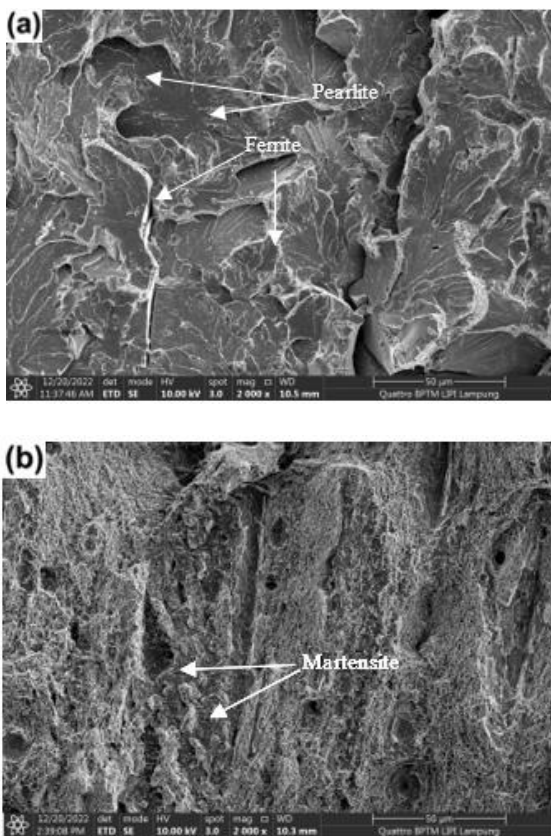


Fig. 4. SEM micrographs showing the impact fracture test results for samples in: (a) FA conditions and (b) SQT condition.

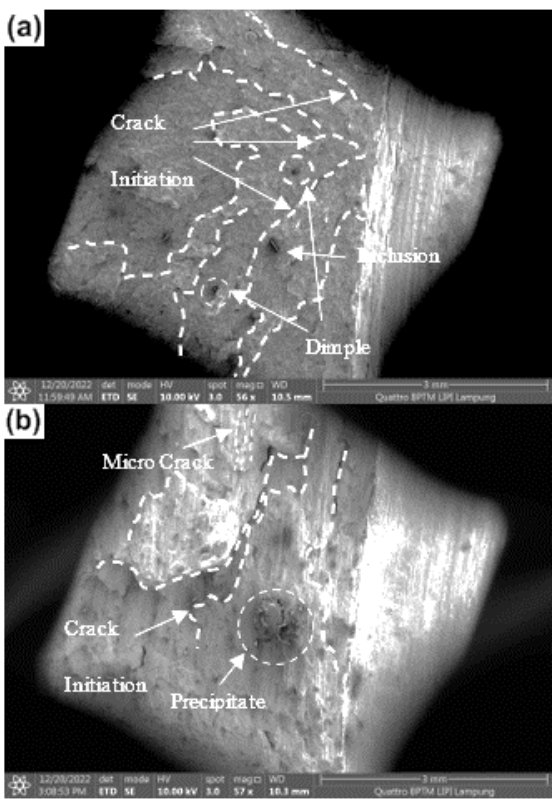
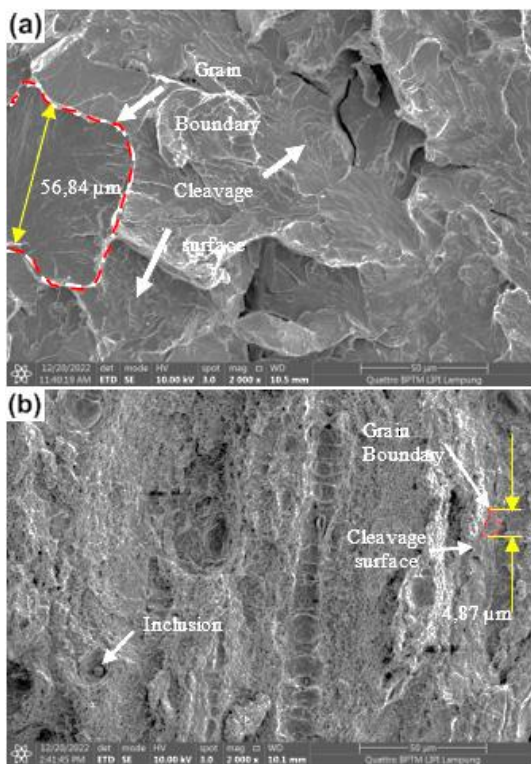


Fig. 5. SEM micrographs showing the fracture directions: (a) FA and (b) SQT heat treatment.



If the observation is carried out at low magnification (2,000x) on the fracture surface there is a cleavage surface in several fault areas. Relatively large grains at low temperatures tend to crack, this is called the cleavage surface. The emergence of a cleavage surface or a pattern like a river flow due to a gradual process, because there is a different orientation in the crack propagation of grain boundary areas. Identification of the initial crack and its growth can be seen through the direction of the cleavage surface grooves which tend to merge towards the local crack growth.

The reason is because the grain size is coarse and large when approaching the surface. Uneven grain size transfer and much larger grains near the surface cause cracking of the inclusions observed on the impact surface indicate that the largest inclusions, usually located within the fine bore, are spherical sulfide particles. In brief, the individual round inclusions that form the fine holes are manganese sulfide.

The presence of voids in the center of the specimen will trigger an unstable compressive failure when the core region of the specimen cannot be longer withstand the applied load. As a result, the JIS SUP 9A specimen was damaged and cracked on its surface due to shear forces forming holes. These results indicate that in this work the most effective inclusions for fracture toughness behavior are sulfide particles.

3.3 EDS analysis

Full Annealing and Single Quenching-Tempering EDS analysis from those observed on the fracture surface at a distance of 1 mm from the notch with 2,000x magnification. The results of this EDS analysis to determine the chemical structure contained in the fault area are as follows:

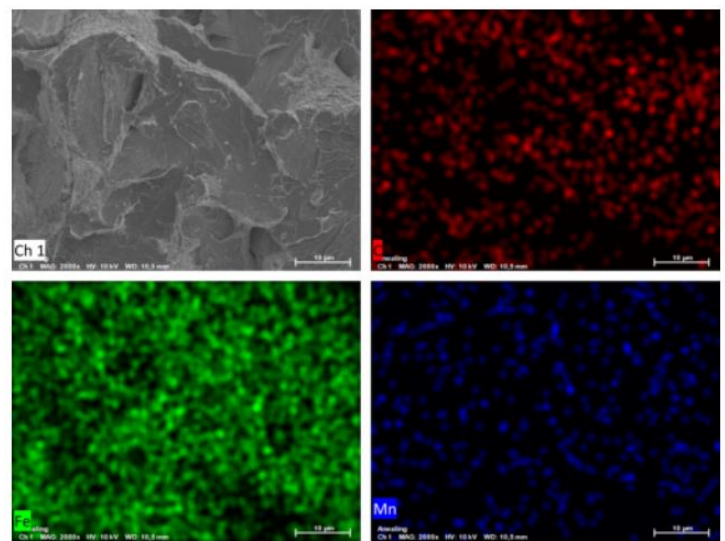


Fig. 7. Full Annealing EDS Mapping analysis with 2,000x magnification at a distance of 1 mm from the notch. Fig. 6. Grain boundary and grain size of treated specimens as a). FA and b). SQT.

It is well known that the fracture process, in low alloy steels, is in such a way that cavities are first formed in the usually largest MnS inclusions, then in smaller oxide inclusions and finally into small carbides [26, 27]. The mean grain size of the SQT specimens was 4.87 μm , about 12 times finer than FA grains (56.84 μm). Confirmation of the crystallographic trend of martensite crystals in the package was obtained from the correlation of more grain sizes with SEM observations [21]. The finer the grain appears, the finer the martensite structure formed during the hardening process, which has an impact on improving the mechanical properties and fracture toughness.

In the graph Fig. 8, the results of the EDS analysis show that the dominant content is contained around the annealing fractography. The graph shows that the Fe content is the largest, which is around 97.55%, then the C content is 1.94% and Mn is 0.51%. In the periodic table of elements of the Xflash SDD Technology Bruker specification, the Fe content is in the shell $K\alpha$: 6.401 $L\alpha$: 0.705, then for Mn it is $K\alpha$: 5.897 $L\alpha$: 0.637 so that the peak lines are close together.

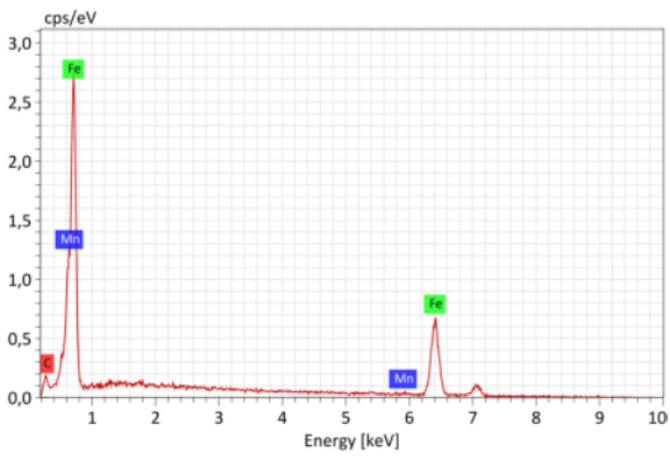


Fig. 8. Graph of EDS Mapping Full Annealing analysis results with 2,000x magnification at a distance of 1 mm from the notch.

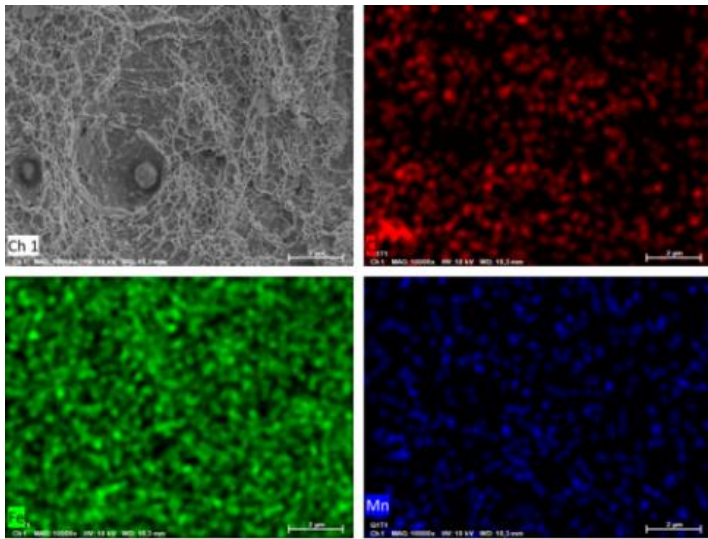


Fig. 9. EDS Mapping Single Quenching-Tempering analysis with 2,000x magnification at a distance of 1 mm from the notch.

Meanwhile, in the EDS analysis of the Single Quenching-Tempering specimen, there are inclusions which are clearly visible on the affected fracture surface, this after analysis shows that the large inclusions which are usually located in the fine dimples are manganese sulfide particles which, although they are oxidizers, affect the formation of martensite, so the tendency will be less in hardness.

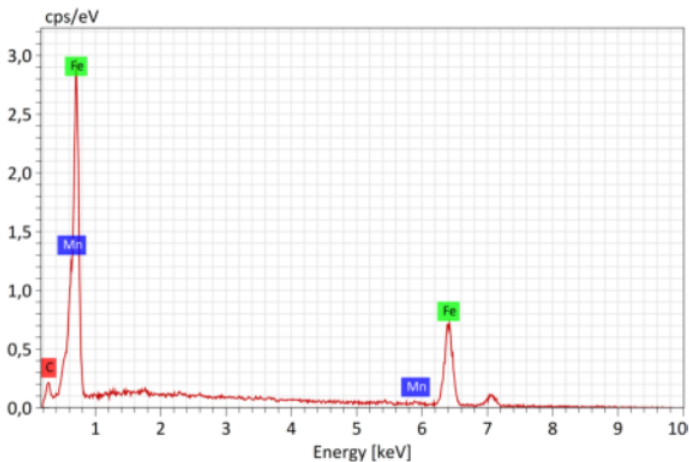


Fig. 10. Graph of EDS Mapping Single Quenching-Tempering analysis results with 2,000x magnification at a distance of 1 mm from the notch.

In Single Quenching-Tempering (SQT) there are inclusions in the form of nucleation during the quenching process. The inclusion images are as follows:

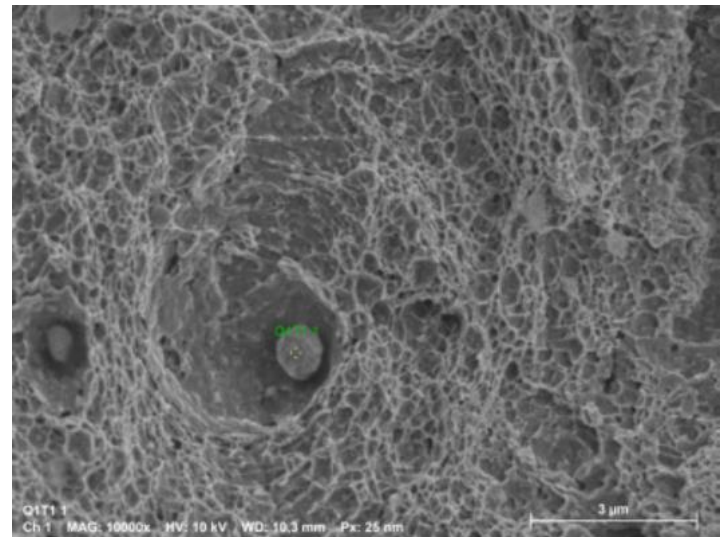


Fig. 11. Globular precipitation-metals element tracking by EDS point analysis formed on the JIS SUP9 steel after SQT processing.

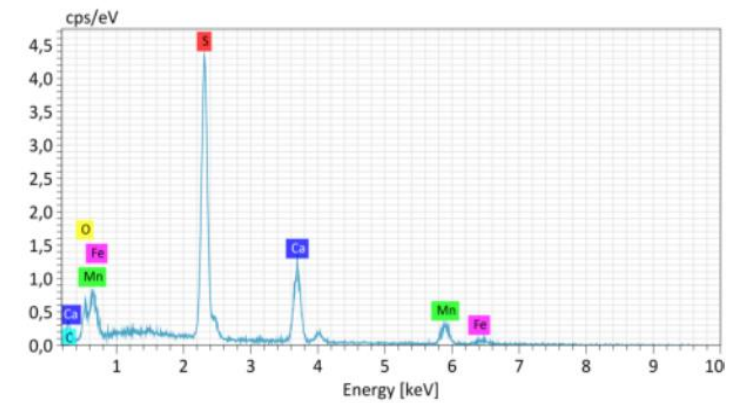


Fig. 12. Graph of EDS Mapping Single Quenching-Tempering analysis results with 10,000x magnification at a distance of 1 mm from the notch

The results of the EDS analysis show that the content of the inclusions formed can be seen in the graph. Inclusions are the cause of failure of a material. The more inclusions occur, the worse the quality of the material. The content in the nucleation inclusions is 7.5% Carbon, 4.9% Carbide, 30.86% Sulfur, 23.03%, Manganese, Iron 5.03%.

4 Conclusion

It knows the effect of Full Annealing (FA) and Single Quenching-Tempering (SQT) heat treatment on the mechanical properties of JIS SUP 9A steel with various tests, such as hardness testing, impact testing, tensile testing, and SEM-EDS. From the test analysis, it can be concluded that the effect of SQT heat treatment increased the value of the material's mechanical properties compared to FA heat treatment. The impact energy value of the SQT heat treatment was 705.2%, higher than FA. Still, the hardness value decreased to 18.8% HRB, which was insignificant because the SQT heat treatment material became ductile. Then the value of the tensile strength of the SQT material increased higher than FA to 16.3%. SEM observations showed that FA heat treatment only had ferrite and pearlite phases while SQT formed martensite, marked with dark-colored areas. The standard deviation values of the 3 UTS scores each have significant deviations, namely FA=14.45 and SQT=12.32. These results indicate that the dominant surface

fracture affects the strength of the steel. Further research development on JIS SUP 9A steel can use the high cycle fatigue test and the low cycle fatigue test, which can see the degree of toughness in a specific duration and the economics of this heat treatment engineering in the use of its derivative products.

Reference

- [1] M. Badaruddin and R. P. Pratama, "Effect of Single and Double Quenching-Tempering Heat Treatments on Microstructures and Tensile Strength of AISI 4140 in Annealing Condition".
- [2] SSAB, "SSAB in brief," *Ssab*, 2020, [Online]. Available: <https://www.ssab.com/company/about-ssab/ssab-in-brief>
- [3] H. K. D. H. Bhadeshia, Professor, S. R. Honeycombe, and Emeritus, *Microstructure and Properties*, 3rd ed., vol. 3, no. 1. London: Butterworth-Heinemann, 2006. [Online]. Available: <https://lib-63vsc6hn5osfsnoz7ztrb6uv.1lib.ph/book/1006801/27b23f>
- [4] C. Ouchi, "Development of steel plates by intensive use of TMCP and direct quenching processes," *ISIJ Int.*, vol. 41, no. 6, pp. 542–553, 2001, doi: 10.2355/isijinternational.41.542.
- [5] C. S. Lee and W. Y. Choo, "Effects of austenite conditioning and hardenability on mechanical properties of B-containing high strength steels," *ISIJ Int.*, vol. 40, no. SUPPL., pp. 189–193, 2000, doi: 10.2355/isijinternational.40.suppl_s189.
- [6] J. Y. YOO, W. Y. CHO, T. W. PARK, and Y. W. KIM, "Microstructures and age hardening characteristics of direct quenched Cu bearing HSLA steel," *ISIJ Int.*, vol. 35, no. 8, pp. 1034–1040, 1995, doi: 10.2355/isijinternational.35.1034.
- [7] Y. Yamada and T. Kuwabara, *Material for Springs*, 1st ed. Springer-Verlag Berlin Heidelberg, 2007. [Online]. Available: <lib-6r2hdtgfpqoh4uxuxqmrsg.1lib.cz/book/2096070/7c9d47>
- [8] H. Chandra, D. K. Pratiwi, and M. Zahir, "High-temperature quality of accelerated spheroidization on SUP9 leaf spring to enhance machinability," *Heliyon*, vol. 4, no. 12, p. e01076, 2018, doi: 10.1016/j.heliyon.2018.e01076.
- [9] V. K. Arora, G. Bhushan, and M. L. Aggarwal, "Fatigue Life Assessment of 65Si7 Leaf Springs: A Comparative Study," *Int. Sch. Res. Not.*, vol. 2014, pp. 1–11, 2014, doi: 10.1155/2014/607272.
- [10] S. Lee, C. Lee, and Y. Cho, "Effect on aqua quenching of spring steel(JIS SUP 9)," *Mater. Sci. Forum*, vol. 566, pp. 249–254, 2008, doi: 10.4028/www.scientific.net/msf.566.249.
- [11] Harry Chandler, *Heat treater's guide: Practices and procedures for irons and steels*, 2nd ed. ASM International, 1995. [Online]. Available: <https://lib-63vsc6hn5osfsnoz7ztrb6uv.1lib.ph/book/1101745/4071bc>
- [12] S.-H. Lee and D.-S. Shim, "Effect of shot peening on fatigue life of heat treated spring steel," *J. Korean Soc. Heat Treat.*, vol. 17, no. 6, pp. 336–341, 2004, [Online]. Available: <https://koreascience.kr/article/JAKO200423943540241.page>
- [13] B. P. Bhardwaj, "The Complete Book on Production of Automobile Components & Allied Products." p. 536, 2014. [Online]. Available: <http://books.google.com/books?id=YgaJAgAAQBAJ&pgis=1>
- [14] X. Tao, C. Li, L. Han, and J. Gu, "Microstructure evolution and mechanical properties of X12CrMoWVNbN10-1-1 steel during quenching and tempering process," *J. Mater. Res. Technol.*, vol. 5, no. 1, pp. 45–57, 2016, doi: 10.1016/j.jmrt.2015.06.001.
- [15] C. Wang, H. Qiu, Y. Kimura, and T. Inoue, "Morphology, crystallography, and crack paths of tempered lath martensite in a medium-carbon low-alloy steel," *Mater. Sci. Eng. A*, vol. 669, pp. 48–57, 2016, doi: 10.1016/j.msea.2016.05.041.
- [16] W. D. Callister and J. Wiley, *Materials Science*, 7th ed., vol. 208, no. 4439. John Wiley & Sons, Inc., 2007. doi: 10.1126/science.208.4439.30.
- [17] Y. Handoyo, "Pengaruh quenching dan tempering pada baja Jis grade S45C terhadap sifat mekanis dan struktur mikro crankshaft," *J. Ilm. Tek. Mesin*, vol. 3, no. 2, pp. 102–115, 2015, [Online]. Available: https://scholar.google.co.id/scholar?hl=id&as_sdt=0%2C5&q=Pengaruh+quenching+dan+tempering+pada+baja+Jis+grade+S45C&btnG=
- [18] ASTM E18-02, "Standard test methods for rockwell hardness and rockwell superficial hardness of metallic materials," *Annu. B. ASTM Stand.*, vol. 01, pp. 1–15, 2005.
- [19] ASTM E8, "ASTM E8/E8M standard test methods for tension testing of metallic materials 1," *Annu. B. ASTM Stand.* 4, vol. 02, no. C, pp. 1–27, 2010, doi: 10.1520/E0008.
- [20] ASTM E 23, "Standard test methods for notched bar impact testing of metallic materials," *Annu. B. ASTM Stand.*, vol. 14, no. 1, pp. 1–26, 2012.
- [21] ASTM E2809-13, *Standard guide for using Scanning Electron Microscopy/X-Ray Spectrometry in forensic paint examinations*. 2003. [Online]. Available: <https://www.astm.org/e2809-13.html>
- [22] B. Laxmi, S. Sharma, J. PK, and A. Hegde, "Quenching oil viscosity and tempering temperature effect on mechanical properties of 42CrMo4 steel," *J. Mater. Res. Technol.*, vol. 16, pp. 581–587, 2022, doi: 10.1016/j.jmrt.2021.11.152.
- [23] A. Saha, D. K. Mondal, and J. Maity, "Effect of cyclic heat treatment on microstructure and mechanical properties of 0.6wt% carbon steel," *Mater. Sci. Eng. A*, vol. 527, no. 16–17, pp. 4001–4007, 2010, doi: 10.1016/j.msea.2010.03.003.
- [24] M. Badaruddin, Sugiyanto, H. Wardono, Andoko, C. J. Wang, and A. K. Rivai, "Improvement of low-cycle fatigue resistance in AISI 4140 steel by annealing treatment," *Int. J. Fatigue*, vol. 125, no. April, pp. 406–417, 2019, doi: 10.1016/j.ijfatigue.2019.04.020.
- [25] S. H. Avner, *Introduction to physical metallurgy*, 2nd ed. McGraw-Hill Inc, 1974. [Online]. Available: <https://lib-63vsc6hn5osfsnoz7ztrb6uv.1lib.ph/book/2712128/41c068>
- [26] Y. Weng, *Ultra-fine grained steels*. Springer, 2009. [Online]. Available: <https://lib-63vsc6hn5osfsnoz7ztrb6uv.1lib.ph/book/594682/c9d994>
- [27] R. Padmanabhan and W. E. Wood, "Microstructural analysis of a multistage heat-treated ultrahigh strength low alloy steel," *Mater. Sci. Eng.*, vol. 66, no. 2, pp. 125–143, 1984, doi: 10.1016/0025-5416(84)90175-7.